# Digital Construction and Characterization of Noise-like Spread Spectrum Signals

Donald C. Buzanowski II, Frederick J. Block, Thomas C. Royster

MIT Lincoln Laboratory

Lexington, MA 02420

*Abstract*—**A new method for generating digital noise-like spread spectrum signals is proposed. A standard binary keystream is used to generate a sequence of chips according to a Gaussian-like chip amplitude distribution for spreading sequences. The properties of these spreading signals are investigated as a function of the number of discrete amplitude levels and number of chips per symbol. The similarities between the generated signals and random Gaussian signals are evaluated based on higher-order moments. Implementation considerations, such as peak-to-average power ratio and amplifier backoff are also considered.**

## I. INTRODUCTION

In order to increase security and capacity, interest has grown in employing signals that are noise-like (e.g., [1]). Direct sequence spread spectrum (DSSS) signals provide benefits such as protection against jamming, low power-spectral density to facilitate coexistence with other systems, and increased difficulty for detection by unauthorized users [2]. Along with the benefits of a traditional direct sequence spread spectrum signal, noise-like DSSS provides improved security as well as additional multiple-access capability in certain cases due to an increased randomness in the signal [3],[4]. However, noise-like signals in general have increased implementation complexity, potentially large peak-to-average power ratios, and non-constant energy per bit.

The effects of these drawbacks vary depending on the construction of the signal. A variety of methods have been proposed to generate these noise-like sequences. A few examples of this include chaotic circuits, m-sequences, and discrete chaotic maps [4],[6]. These methods for generating pseudorandom noise sequences can produce a variety of output distributions based on their parameters. In some cases these chaotic sequences can generate large numbers of sequences all with low cross-correlations making them ideal for achieving increased capacity [6].

In this paper, a method for digital construction of multi-amplitude direct sequence spread spectrum signals is proposed. The realization of amplitude sequences is driven by a standard binary keystream. The amplitude distribution used with this method is arbitrary; however, we focus on a set of chip amplitudes which approximate a Gaussian normal distribution.

This paper is organized as follows. In Section II, a description is provided of the process of creating an approximation of a Gaussian normal distribution through the use of binomial random variables. Sequence generation is also described. In Section III, methods of statistically testing the model are described. In Section IV, implementation considerations, such as peak-to-average power ratio and amplifier distortion are discussed. In Section V, the bit error rate performance is evaluated parametrically based on the amplitude distribution and number of chips per bit. Multiple-access interference performance is also considered. Conclusions are provided in Section VI.

## II. DISCRETE GAUSSIAN MODEL

### A. Constructing the Model

We begin with the process of generating the chip amplitude distribution. The transmitted signal for $b_m$, the $m$th information bit is as follows

$$s_m(t) = (-1)^{b_m} \sum_{i=0}^{K-1} a_{i,m}, \qquad (1)$$

where $a_{i,m}$ is the $i$th chip of the spreading sequence for the $m$th bit and there are $K$ chips per bit. In general, each chip of the spreading sequence can take on one of $N$ possible amplitudes. The $k$th amplitude, $a_k$, occurs with probability $p_k$. Any desired amplitude set and probability distribution can be employed by this model. Our focus is on an amplitude set and probability distribution that approximates a zero-mean Gaussian process.

To determine the values of $p_k$ that approximate a Gaussian distribution, a binomial distribution with parameters $n = N$ and $p = 1/2$ is employed. The probability that the $k$th amplitude value is chosen for a chip is given by the standard expression for the Binomial probability mass function, provided in (2) for convenience

$$P(X = k) = \binom{n}{k} p^k (1-p)^{n-k}. \qquad (2)$$

An example of the process for determining the values of $a_k$ is provided in Figure 1(a) for $N = 4$ levels. The probability distribution function of a Guassian random variable is partitioned such that the expected vaule of the $i$th partition is equal to $p_i$. In particular, the boundaries of each of these partitioned regions, $a_R$ and $b_R$, are determined using the
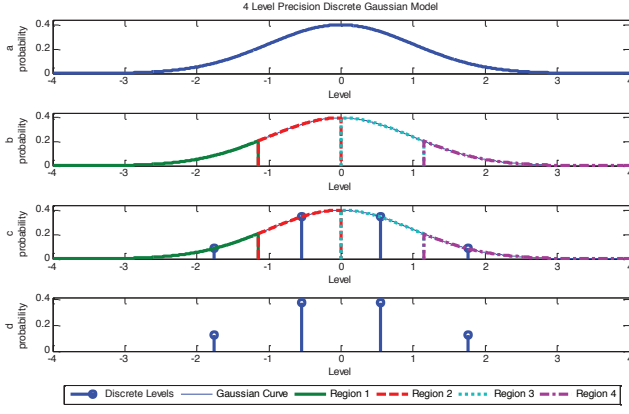
Fig. 1. Four-level precision discrete Gaussian model construction.



Fig. 2. Example Gaussian-like spreading sequences.

inverse Q function. An example of the partitions is shown in Figure 1(b) for four levels. The amplitude $a_i$ is then set to the expected value of the $i$th partition, as illustrated in Figures 1(c) and 1(d). If the variance of the resulting discrete distribution is not $\sigma^2 = 1$ (e.g., for small values of $N$), the set of amplitudes is linearly scaled such that $\sigma^2 = 1$.

*B. Generating the Sequence*

Spreading sequences are generated starting with a pseudo-random binary sequence in which 0 and 1 are equiprobable. Such sequences are typically employed in cryptographically-driven transmission security (TRANSEC) functions. For an $N$-level sequence, each group of $N-1$ bits from the pseudoran-dom sequence is summed. The result is a value $k$ between 0 and $N-1$, which is Binomially distributed. The result specifies the amplitude level $a_k$ of the current chip. An example of chipping sequences generated for $N = 2$, 4, 16, and 256 levels of precision are shown in Figure 2. Note that while this approach enables the Gaussian-like chip distribution to be generated with a traditional key stream generator, the rate of the key stream must be a factor of $(n-1)K/r$ higher than the system's bit rate, where $K$ is the spreading factor and $r$ is the rate of the error-control code.

## III. GAUSSIAN MODEL STATISTIC

To determine the suitability of employing the proposed method for generating Gaussian-like signals, the mean $\mu$, variance $\sigma^2$, skewness $\gamma$, and kurtosis $\kappa$ are evaluated. The four corresponding expressions are as follows

$$\mu = \frac{1}{N} \sum_{i=0}^{N-1} x_i \tag{3}$$

$$\sigma^2 = \frac{1}{N-1} \sum_{i=0}^{N-1} x_i^2 \tag{4}$$

$$\gamma = \frac{m_3}{m_2^{3/2}} = \frac{\frac{1}{n} \sum_{i=0}^{N-1} (a_i - \mu)^3}{\left(\frac{1}{n} \sum_{i=0}^{N-1} (a_i - \mu)^2\right)^{3/2}} \tag{5}$$
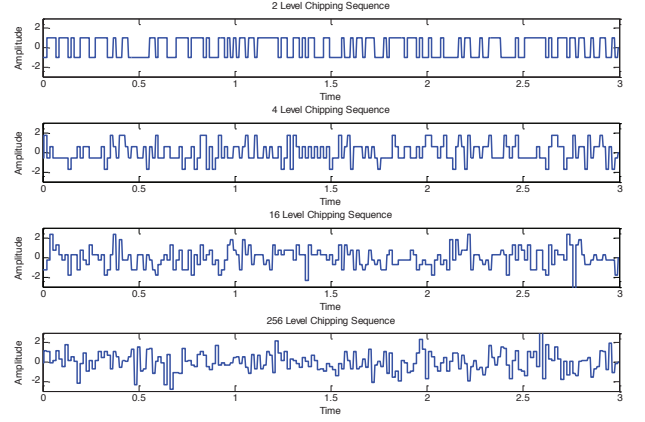
$$\kappa = \frac{n(n+1)(n-1)}{(n-2)(n-3)} \frac{\sum_{i=0}^{N-1} (x_i - \mu)^4}{\left(\sum_{i=1}^{n} (x_i - \mu)^2\right)^2}. \tag{6}$$

Skewness an indicator of the level and direction of skew in the data and kurtosis an indicator of the shape of the data, peaked or flat. As illustrated in Figure 3, the values of mean, variance and skewness were found to be constant for any number of levels $N$. Mean and skewness maintained a value of 0, which is expected due to the symmetrical nature of a Gaussian normal distribution. Variance maintained a value of 1 by design. The value for kurtosis increases as a function of $N$ and eventually approaches a value of 3, which matches the kurtosis of a Gaussian normal distribution. The value of $N$ at which the kurtosis of the model reached 3 occurs at approximately 16. Based on the statistical analysis, the proposed method successfully modeled a Gaussian normal distribution and had exceptional statistics at any value of $N$ greater than 15 levels.

## IV. IMPLEMENTATION CONSIDERATIONS

Considering the variation in amplitude of the generated sequences for $N > 2$, the peak to average power ratio must be considered in the system implementation, as amplifier distortion could potentially distort the signal and degrade the Gaussian-like nature of the signals. Given a continuous-time transmitted signal, the peak and average signal power levels are

$$P_p = \max(A^2(t)) \tag{7}$$

$$P_a = T^{-1} \int_0^T A^2(t)\mathrm{dt}, \tag{8}$$

respectively, and the peak-to-average power ratio is $P_p/P_a$.

To evaluate the impact of amplifier distortion, it is of interest to determine the kurtosis of the output signal as a function of amplifier output backoff (OBO), where OBO is the
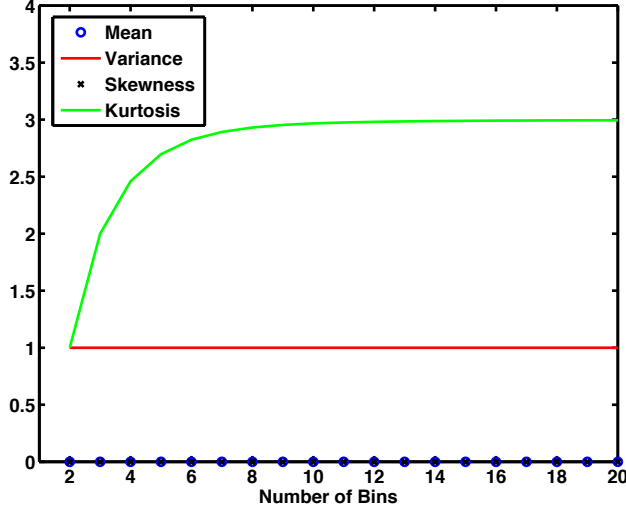
Fig. 3. Gaussian model testing as a function of number of discrete levels.



Fig. 4. Observed signal kurtosis as a function of amplifier output back off.

amount by which the output power of the amplifier is decreased relative to its maximum value. Larger values of OBO typically provide larger ranges in which signals with nonzero peak-to-average power ratios can be linearly amplified. On the other hand, larger values of OBO provide reduced average transmit power and can degrade the bit error rate performance of the link.

In an actual implementation, two independent streams of the signal described in (1) would be transmitted, one on the inphase branch and the other on the quadrature branch. The amplifier performance corresponding to such complex noise-like signals is determined using a representative AM/AM and AM/PM amplifier model. In particular, the complex input signal is input to the amplifier and the kurtosis of the corresponding complex output signal is computed. To determine the kurtosis of a complex signal, a modified version of the kurtosis, here called the *Normalized Complex Kurtosis*, is used and given by [8]

$$\kappa' = \frac{\frac{1}{N}\sum_{i=0}^{N-1}|x_i|^4 - \frac{2}{N^2}(\sum_{i=0}^{N-1}|x_i|^2)^2 - \frac{1}{N^2}|\sum_{i=0}^{N-1}x_i^2|^2}{\sigma^4}.$$

(9)

Note that with this formulation, Gaussian signals exhibit a value of zero. For the remainder of the paper, the measure given in (9) will be referred to as simply "Kurtosis." Kurtosis results are provided in Figure 4 for detectors operating at two different values of detector $E_c/N_0$. Results for binary signaling and multilevel signaling are provided as well, and the kurtosis value for binary signaling does not change as a function of OBO, since the constant-magnitude binary modulation undergoes minimal distortion by the amplifier. At low OBO values, the multilevel signals experience significant amplitude distortion and achieve the same kurtosis value as for binary signaling. As OBO increases, kurtosis increases as well. Values of OBO
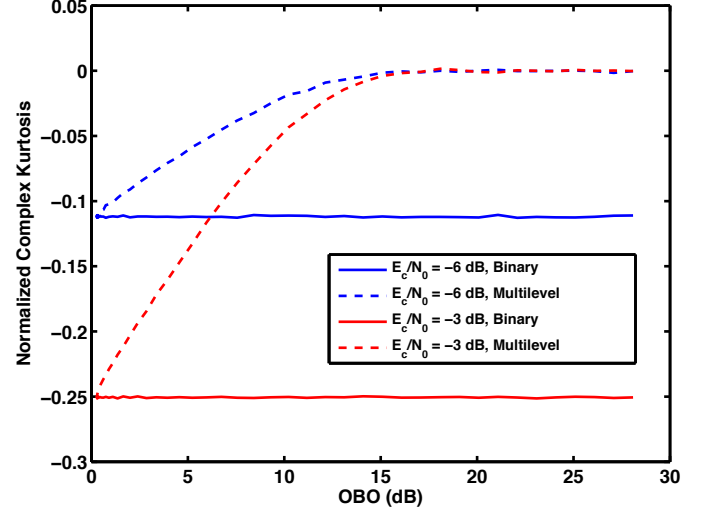
approximately 15 dB are required to maintain a kurtosis value at the level of a true complex Gaussian signal.

## V. PERFORMANCE

### A. AWGN performance

The performance of these signals with $K = 2L$ chips per bit can be approximated by the bit error rate of a link operating over $L$ resolvable Rayleigh fading paths and optimal combining. This is because both the signal and matched filter have Gaussian distributed amplitudes, and when the received sequence and matched filter are aligned, the result is a sum of squared Gaussian amplitudes. The theoretical expression for bit error rate is given by [7]

$$P_b = \left[\frac{1}{2}(1-\nu)\right]^L \sum_{k=0}^{L-1}\binom{L-1+k}{k}\left[\frac{1}{2}(1+\nu)\right]^k,$$

(10)

where $\nu = \sqrt{\bar{\gamma}_c/(1+\bar{\gamma}_c)}$ and $\bar{\gamma}_c = (E_s/N_0)E(a_k^2)$.

Of course, when $N = 2$, there is no variation in the magnitude of the amplitude, so the standard expression for bit error rate for BPSK in AWGN applies. The expression in (10) is intended for use with larger values of $N$. To determine the accuracy of these bounds as a function of $N$ and $K$, a link employing the Gaussian model was simulated.

In Figure 5, the discrete simulated values of $E_b/N_0$ required for a bit error probability of $4\%$ is plotted as a function of $K$, the number of chips per bit, for $N = 4$ and $N = 32$ bins. The analytical expression of (10) is also plotted. The accuracy of the analytical expression is seen to be better for larger values of $N$, which is because the actual signal is more Gaussian-like and thus the expression is more applicable. For values of chips per bit of 8 and above, the results of the analytical expression match exactly those of the simulations.
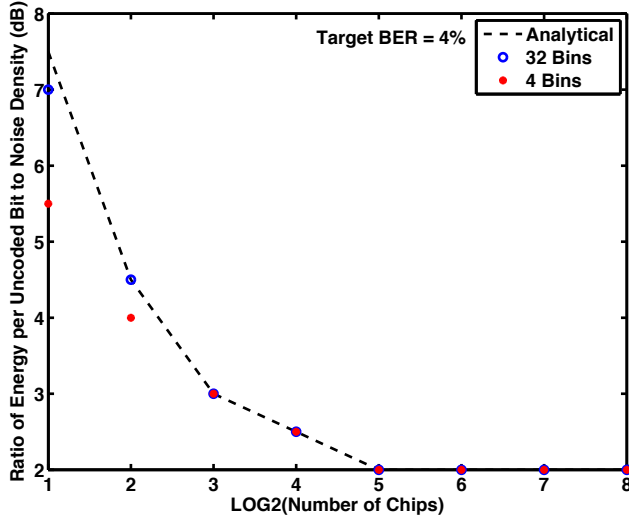
3

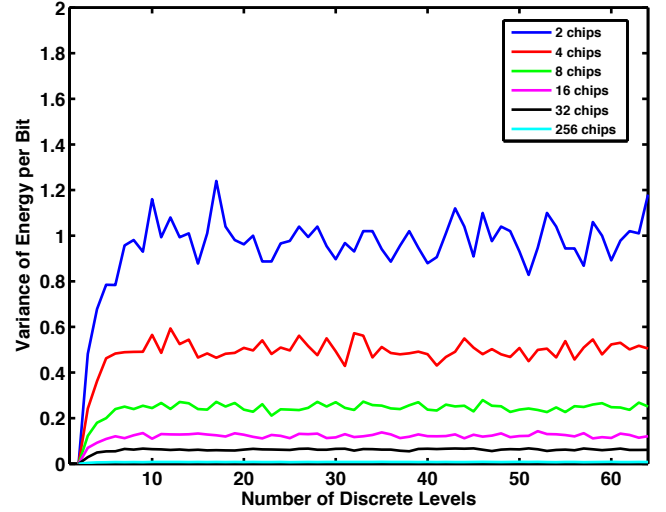Fig. 5. Value of $E_b/N_0$ required for 4% bit error rate.



Fig. 7. Variance of energy per bit for various numbers of chips per bit and discrete chip amplitude levels.
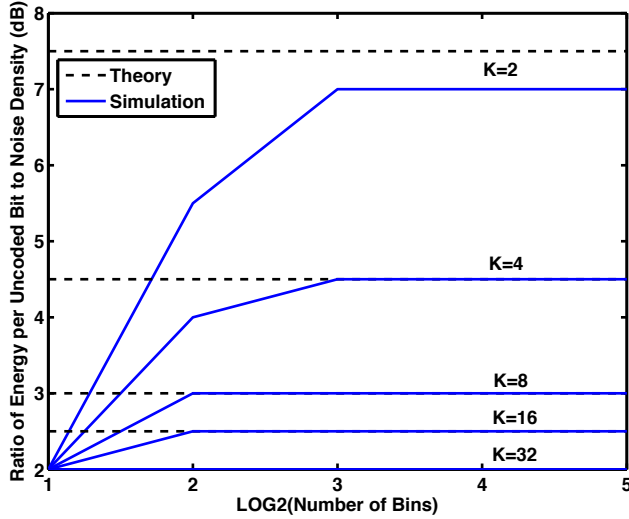


Fig. 6. Value of $E_b/N_0$ required for 4% bit error rate.

The results of a similar trade between $E_b/N_0$ and the number of bins are illustrated in Figure 6. For $K = 32$ chips per bit, the performance matches that of ideal BPSK regardless of the number of bins. For fewer chips per bit, the analytical expression predicts a fixed loss in performance relative to ideal BPSK. The actual performance trends can be seen from the simulation data. For a given number of chips per bit, a relatively low value of bins is required for the performance to match that of the analytical expression.

Because of the variation of performance depending on the number of chips per symbol, the distribution of energy per bit was examined. Clearly, it is infeasible to have a constant energy per bit with non-constant power per chip and only a few chips per bit. Using (5) the variance of bit energy was examined.

Simulation results are presented in Figure 7 that provide an illustration of the variance in bit energy as a function of $N$ for various numbers of chips per bit. As expected, regardless of the number of chips per bit, if there are only two levels then the variance is zero. For $N > 2$ levels, maintaining a low variance requires a large number of chips per bit. These results mimic the trend discussed for bit error rate simulations.

Another method for combating varying energy per bit is to vary bit duration based on bit energy. Varying bit duration adds another level of complexity to the signal which may result in increased security [3].

### B. Multiple-Access Interference

It is of interest to determine the effect of non-constant chip magnitudes on multiple-access interference. For a traditional DSSS system ($N = 2$), the chip magnitudes are constant, so as long as the average power $I$ of an interfering user does not exceed the average power $S$ of the desired user, the performance of the desired user does not degrade in the absence of noise. We define the quantity SIR as the ratio $S/I$ in dB. For $N > 2$, because of the peak-to-average power ratio larger than unity, the performance of the desired user can degrade even for values of SIR $> 0$.

Simulation results are presented in Figure 8 for the minimum SIR required to achive a bit error rate of $10^{-3}$ for various values of $N$ and chips per bit. For small values of chips per bit, the required SIR increases as a function of the number of amplitude levels $N$. This results from the large variance in energy per bit, as previously described. As chipping rates are increased the dependence on performance as a function of $N$ is reduced. Based on results, for values of chips per bit at least 16 there is minimal SIR degradation, and the degradation is eliminated for 64 or greater chips per bit.
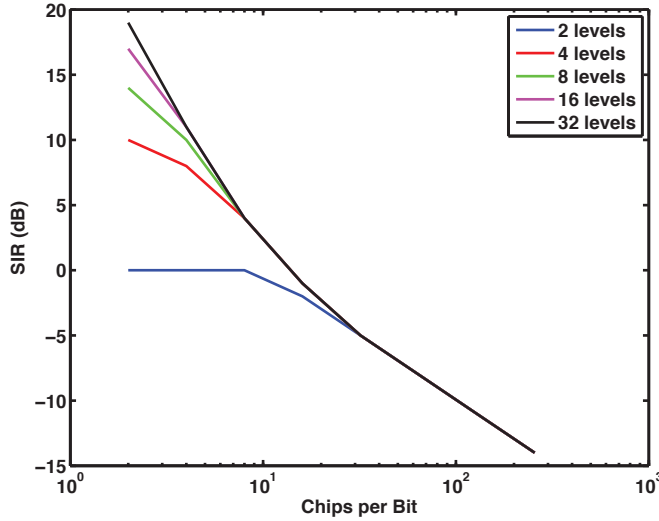
Fig. 8. SIR (dB) required for a $10^{-3}$ bit error probability.

Further work is planned in this area for the final paper, for which we will compute performance for larger numbers of simultaneous signals.

## VI. CONCLUSION

A method for constructing noise-like spread spectrum signals was described. This method was employed to produce sequences with Gaussian-like amplitude distributions, though the method is more generally applicable and can be used to generate chip sequences according to any probability and amplitude distribution. The Gaussian-like sequences were evaluated based on several metrics, including fit to Gaussian statistics, peak-to-average power ratio, bit error rate, performance under multiple-access interference.

With appropriate parameters, this model successfully approximated a Gaussian normal distribution and was extremely accurate for 16 or more amplitude levels. Because of non-constant chip magnitudes, peak to average power ratios were larger than unity. For practical systems, the impact of amplifier distortion must be considered, and increased distortion was observed in some cases. To maintain the fit to Gaussian statistics, the required amplifier backoff levels were computed.

Simulation results for bit error rate versus average signal energy to thermal noise ratio showed increased bit error rates for higher precision models at higher power ratios. The non-constant energy per bit caused this increase in bit error rates. Bit energy distributions were examined and trends were consistent between the value of variance and the bit error rate for various levels of chipping rates. By increasing the number of chips per bit to approximately 32 or greater, bit error rates approached theoretical values for BPSK modulation. At the same time variance levels for bit energy approached zero.

A multiple-access interference scenario was evaluated for several parameter sets. Although the non-constant chip magni-tudes can cause performance degradation relative to traditional constant-magnitude DSSS, it was found that bit error rates approached the traditional DSSS bit error rates for 16 or greater chips per bit. The performance reduction is eliminated for chipping rates of 64 or greater.

Overall the system was shown to exhibit statistics similar to that of a Gaussian normal distribution which can be used to approximate white noise. Various characteristics of the model were discussed and shown to result in similar functionality to traditional direct sequence spread spectrum at certain levels of operation. Through added randomness the proposed system successfully generated a noise-like signal which can be shown to increase security and capacity under various circumstances [6].

## REFERENCES

[1] Michaels, A. J., and Chester, D. B., "Efficient and flexible chaotic communication waveform family," *IEEE Military Communications Conference*, 2010

[2] Pursley, M.B., "Direct-sequence spread-spectrum communications for multipath channels," *IEEE Transactions on Microwave Theory and Techniques*, vol.50, no.3, pp.653,661, Mar 2002.

[3] Riaz, A; Ali, M., "Chaotic Communications, their applications and advantages over traditional methods of communication," *6th International Symposium on Communication Systems, Networks and Digital Signal Processing (CNSDSP)*, pp. 21–25, July 2008.

[4] Chen, C.-C.; Yao, K.; Umeno, K.; Biglieri, Ezio, "Design of spread-spectrum sequences using chaotic dynamical systems and ergodic theory," *IEEE Transactions on Circuits and Systems I: Fundamental Theory and Applications*, vol.48, no.9, pp.1110–1114, Sep 2001.

[5] Nguyen Xuan Quyen, Vu Van Yem, and Thang Manh Hoang, "A Chaos-Based Secure Direct-Sequence/Spread-Spectrum Communication System," *Abstract and Applied Analysis*, vol. 2013, Article ID 764341, 11 pages, 2013.

[6] Heidari-Bateni, G.; McGillem, C.D., "Chaotic sequences for spread spectrum: an alternative to PN-sequences," *IEEE International Conference on Selected Topics in Wireless Communications*, pp.437–440, Jun 1992.

[7] J. G. Proakis, *Digital Communications* (5th ed.), New York: McGraw Hill, 2008.

[8] Mathis, H, "On the kurtosis of digitally modulated signals with timing offsets," *Third IEEE Signal Processing Workshop on Signal Processing Advances in Wireless Communications*, Mar 2001.